

Present status and future prospects for a Higgs boson discovery at the Tevatron and LHC

Howard E. Haber

Santa Cruz Institute for Particle Physics
University of California, Santa Cruz, CA 95064 USA

E-mail: haber@scipp.ucsc.edu

Abstract. Discovering the Higgs boson is one of the primary goals of both the Tevatron and the Large Hadron Collider (LHC). The present status of the Higgs search is reviewed and future prospects for discovery at the Tevatron and LHC are considered. This talk focuses primarily on the Higgs boson of the Standard Model and its minimal supersymmetric extension. Theoretical expectations for the Higgs boson and its phenomenological consequences are examined.

1. Introduction

The origin of electroweak symmetry breaking and the mechanism that generates the masses of the known fundamental particles is one of the central challenges of particle physics. The Higgs mechanism [1] in its most general form can be used to explain the observed masses of the W^\pm and Z bosons as a consequence of three Goldstone bosons (G^\pm and G^0) that end up as the longitudinal components of the massive gauge bosons. These Goldstone bosons are generated by the underlying dynamics responsible for electroweak symmetry breaking. However, the fundamental nature of this dynamics is still unknown. Two broad classes of electroweak symmetry breaking mechanisms have been pursued theoretically. In one class of theories, the electroweak symmetry breaking dynamics is weakly-coupled, while in the second class of theories the dynamics is strongly-coupled [2].

The electroweak symmetry breaking dynamics of the Standard Model (SM) employs a self-interacting complex doublet of scalar fields, which consists of four real degrees of freedom [3]. Elementary scalar dynamics yields a non-zero scalar field vacuum expectation value (vev), which leads to the breaking of the electroweak symmetry. Consequently, three massless Goldstone bosons are generated, while the fourth scalar degree of freedom that remains in the physical spectrum is the CP-even neutral Higgs boson of the Standard Model. Precision electroweak data favors a Higgs mass below 200 GeV, in which case the scalar self-interactions are weak [4, 5]. In the weakly-coupled approach to electroweak symmetry breaking, the Standard Model is very likely embedded in a supersymmetric theory [6] in order to stabilize the large gap between the electroweak and the Planck scales in a natural way [7]. The minimal supersymmetric extension of the Standard Model (MSSM) employs two complex Higgs doublets, resulting in five physical scalar degrees of freedom. In a large range of the MSSM parameter space, the properties of the lightest scalar of the MSSM are nearly indistinguishable from those of the SM Higgs boson.

It is possible that the dynamics responsible for electroweak symmetry breaking is strongly-coupled [8]. Precision electroweak data disfavors the simplest classes of models based on this approach. Nevertheless, it remains possible that the physics of electroweak symmetry breaking is more complicated than suggested by the Standard Model or its supersymmetric extensions. However, in this talk I will not consider these theoretical alternatives nor their phenomenological consequences.

2. Theory of weakly-coupled Higgs bosons

2.1. The Standard Model Higgs Boson

In the Standard Model, the Higgs mass is given by: $m_h^2 = \frac{1}{2}\lambda v^2$, where λ is the Higgs self-coupling parameter. Since λ is unknown at present, the value of the Standard Model Higgs mass is not predicted. In contrast, the Higgs couplings to fermions [bosons] are predicted by the theory to be proportional to the corresponding particle masses [squared-masses]. In particular, the SM Higgs boson is a CP-even scalar, and its couplings to gauge bosons, Higgs bosons and fermions are given by:

$$\begin{aligned} g_{hff} &= \frac{m_f}{v}, & g_{hVV} &= \frac{2m_V^2}{v}, & g_{hhVV} &= \frac{2m_V^2}{v^2}, \\ g_{hhh} &= \frac{3}{2}\lambda v = \frac{3m_h^2}{v}, & g_{hhhh} &= \frac{3}{2}\lambda = \frac{3m_h^2}{v^2}, \end{aligned} \quad (1)$$

where $V = W$ or Z and $v = 2m_W/g = 246$ GeV. In Higgs production and decay processes, the dominant mechanisms involve the coupling of the Higgs boson to the W^\pm , Z and/or the third generation quarks and leptons. Note that a h^0gg coupling (g =gluon) is induced by virtue of a one-loop graph in which the Higgs boson couples dominantly to a virtual $t\bar{t}$ pair. Likewise, a $h^0\gamma\gamma$ coupling is generated, although in this case the one-loop graph in which the Higgs boson couples to a virtual W^+W^- pair is the dominant contribution. Further details of the SM Higgs boson properties are given in ref. [3]. Reviews of the SM Higgs properties and its phenomenology, with an emphasis on the impact of loop corrections to the Higgs decay rates and cross-sections can be found in Refs. [9, 10, 11].

2.2. Extended Higgs sectors

For an arbitrary Higgs sector, the tree-level ρ -parameter is given by [12]

$$\rho_0 \equiv \frac{m_W^2}{m_Z^2 \cos^2 \theta_W} = 1 \quad \iff \quad (2T + 1)^2 - 3Y^2 = 1, \quad (2)$$

independently of the Higgs vevs, where T and Y specify the weak-isospin and the hypercharge of the Higgs representation to which it belongs. Y is normalized such that the electric charge of the scalar field is $Q = T_3 + Y/2$. The simplest solutions are Higgs singlets $(T, Y) = (0, 0)$ and hypercharge-one complex Higgs doublets $(T, Y) = (\frac{1}{2}, 1)$. Thus, we shall consider non-minimal Higgs sectors consisting of multiple Higgs doublets (and perhaps Higgs singlets), but no higher Higgs representations, to avoid the fine-tuning of Higgs vevs.

The two-Higgs-doublet model (2HDM) consists of two hypercharge-one scalar doublets. Of the eight initial degrees of freedom, three correspond to the Goldstone bosons and five are physical: a charged Higgs pair, H^\pm and three neutral scalars. In contrast to the SM where the Higgs-sector is CP-conserving, the most general 2HDM allows for Higgs-mediated CP-violation (see ref. [13] for a complete specification of the 2HDM tree-level interactions). If CP is conserved,

the Higgs spectrum contains two CP-even scalars, h^0 and H^0 and a CP-odd scalar A^0 . Thus, new features of the extended Higgs sector include: (i) charged Higgs bosons; (ii) a CP-odd Higgs boson (if CP is conserved in the Higgs sector); (iii) possible Higgs-mediated CP-violation and neutral Higgs states of indefinite CP. More exotic Higgs sectors allow for doubly-charged Higgs bosons, etc. Further details of extended Higgs sectors can be found in ref. [3].

2.3. The Higgs sector of the MSSM

The Higgs sector of the MSSM is a 2HDM, whose Yukawa couplings and Higgs potential are constrained by supersymmetry (SUSY). Minimizing the Higgs potential, the neutral components of the Higgs fields acquire vevs v_u and v_d , where $v^2 \equiv v_d^2 + v_u^2 = 4m_W^2/g^2 = (246 \text{ GeV})^2$. The ratio of the two vevs is an important parameter of the model, $\tan \beta \equiv v_u/v_d$. The five physical Higgs particles consist of a charged Higgs pair H^\pm , one CP-odd scalar A^0 , and two CP-even scalars h^0, H^0 , obtained by diagonalizing the 2×2 CP-even Higgs squared-mass matrix. All tree-level Higgs masses and couplings and the angle α (which parameterizes the diagonalization of the 2×2 CP-even Higgs squared-mass matrix) can be expressed in terms of two Higgs sector parameters, usually chosen to be m_A and $\tan \beta$. See refs. [10, 14] for further details.

At tree level, $m_h \leq m_Z |\cos 2\beta| \leq m_Z$, which is ruled out by LEP data. But, this inequality receives quantum corrections. The tree-level Higgs mass is shifted due to an incomplete cancellation of particles and their superpartners (which would be an exact cancellation if supersymmetry were unbroken) that contribute at one-loop to the Higgs self-energy function. The Higgs mass upper bound is then modified to [15]

$$m_h^2 \lesssim m_Z^2 + \frac{3g^2 m_t^4}{8\pi^2 m_W^2} \left[\ln \left(\frac{M_S^2}{m_t^2} \right) + \frac{X_t^2}{M_S^2} \left(1 - \frac{X_t^2}{12M_S^2} \right) \right], \quad (3)$$

where $X_t \equiv A_t - \mu \cot \beta$ governs stop mixing and M_S^2 is the average top-squark squared-mass. The state-of-the-art computation includes the full one-loop result, all the significant two-loop contributions, some of the leading three-loop terms, and renormalization-group improvements [16]. The final conclusion is that $m_h \lesssim 130 \text{ GeV}$ [assuming that the top-squark mass is no heavier than about 2 TeV]. This upper bound is reached when $\tan \beta \gg 1$ and $m_A \gg m_Z$ in the so-called *maximal mixing scenario*, which corresponds to choosing $X_t/M_S \sim 2$ so that the predicted value of m_h is maximal.

Tree-level couplings of the MSSM Higgs bosons with gauge bosons are often suppressed by an angle factor, either $\cos(\beta - \alpha)$ or $\sin(\beta - \alpha)$, as shown in the table below.

<u>$\cos(\beta - \alpha)$</u>	<u>$\sin(\beta - \alpha)$</u>	<u>angle-independent</u>
$H^0 W^+ W^-$	$h^0 W^+ W^-$	—
$H^0 Z Z$	$h^0 Z Z$	—
$Z A^0 h^0$	$Z A^0 H^0$	$Z H^+ H^-$, $\gamma H^+ H^-$
$W^\pm H^\mp h^0$	$W^\pm H^\mp H^0$	$W^\pm H^\mp A^0$

Tree-level Higgs-fermion couplings may be either suppressed or enhanced with respect to the SM value, $gm_f/2m_W$. The charged Higgs boson couplings to fermion pairs, with all particles pointing into the vertex, are:

$$g_{H^- t \bar{b}} = \frac{g}{\sqrt{2}m_W} \left[m_t \cot \beta P_R + m_b \tan \beta P_L \right],$$

$$g_{H^- \tau^+ \nu} = \frac{g}{\sqrt{2}m_W} \left[m_\tau \tan \beta P_L \right],$$

where $P_{R,L} \equiv \frac{1}{2}(1 \pm \gamma_5)$, and the neutral Higgs boson couplings are:

$$\begin{aligned}
h^0 b\bar{b} \quad (\text{or } h^0 \tau^+ \tau^-) : & \quad -\frac{\sin \alpha}{\cos \beta} = \sin(\beta - \alpha) - \tan \beta \cos(\beta - \alpha), \\
h^0 t\bar{t} : & \quad \frac{\cos \alpha}{\sin \beta} = \sin(\beta - \alpha) + \cot \beta \cos(\beta - \alpha), \\
H^0 b\bar{b} \quad (\text{or } H^0 \tau^+ \tau^-) : & \quad \frac{\cos \alpha}{\cos \beta} = \cos(\beta - \alpha) + \tan \beta \sin(\beta - \alpha), \\
H^0 t\bar{t} : & \quad \frac{\sin \alpha}{\sin \beta} = \cos(\beta - \alpha) - \cot \beta \sin(\beta - \alpha), \\
A^0 b\bar{b} \quad (\text{or } A^0 \tau^+ \tau^-) : & \quad \gamma_5 \tan \beta, \\
A^0 t\bar{t} : & \quad \gamma_5 \cot \beta,
\end{aligned}$$

where the γ_5 indicates a pseudoscalar coupling. Especially noteworthy is the possible $\tan \beta$ -enhancement of certain Higgs-fermion couplings. Typically, $1 \lesssim \tan \beta \lesssim m_t/m_b$ in most MSSM models.

2.4. The decoupling limit

In many models with extended Higgs sectors, a parameter regime exists in which one Higgs boson is light (of order m_Z) and all other Higgs scalars are very heavy ($\gg m_Z$). In this case, one can formally integrate out the heavy scalar states. The effective low-energy Higgs theory is precisely that of the SM Higgs boson. This is called the decoupling limit [17]. The MSSM exhibits the decoupling limit for $m_A \gg m_Z$. In this case, it is easy to verify that $m_A \simeq m_H \simeq m_{H^\pm}$, up to corrections of $\mathcal{O}(m_Z^2/m_A)$, and $\cos(\beta - \alpha) = 0$ up to corrections of $\mathcal{O}(m_Z^2/m_A^2)$. Examining the Higgs couplings listed above, one can check that in the limit of $\cos(\beta - \alpha) \rightarrow 0$, all h^0 couplings to SM particles approach their SM limits, as expected.

3. Present status of the Higgs boson

3.1. Direct Higgs mass bounds

From 1989–2000, experiments at LEP searched for $e^+e^- \rightarrow Z \rightarrow h^0 Z$ (where one of the Z -bosons is on-shell and one is off-shell). No significant evidence was found leading to a lower bound on the Higgs mass, $m_h > 114.4$ GeV at 95% CL [18]. Recent data from the Tevatron extends the disallowed Higgs mass region by excluding $158 \text{ GeV} < m_h < 175 \text{ GeV}$ at 95% CL [19].

The MSSM Higgs mass bounds are more complicated, since they depend on a variety of MSSM parameters. Since supersymmetric radiative corrections to the lightest MSSM Higgs mass must be significant to avoid exclusion, the MSSM Higgs mass bounds depend sensitively on the multi-dimensional MSSM parameter space. In the maximal-mixing scenario, the LEP Higgs search rules out (at 95% CL) charged Higgs bosons with $m_{H^\pm} < 79.3$ GeV and neutral Higgs masses with $m_h < 92.9$ GeV and $m_A < 93.4$ GeV [20]. In certain other scenarios, it is possible to significantly relax these bounds. For example, in the CPX scenario [21], supersymmetric radiative corrections introduce CP-violating phenomena into the MSSM Higgs sector, in which case an arbitrarily light Higgs boson is still allowed for $3 \lesssim \tan \beta \lesssim 10$ [22].

3.2. Indirect Higgs mass bounds

Precision electroweak data puts indirect bounds on the Higgs mass. One can fit a plethora of electroweak observables, based on the predictions of the SM, in which the Higgs mass is allowed to float. The global fit of precision electroweak data yields a χ^2 distribution for the goodness of

fit as a function of the Higgs mass. If the direct Higgs search bounds are omitted, the favored central value of the Higgs mass obtained by the LEP Electroweak Working group is 89 GeV, with a one-sigma experimental uncertainty of +35 and -26 GeV [4]. The corresponding one-sided 95% CL upper bound excludes $m_h < 158$ GeV. Including the LEP Higgs search data, the upper bound increases to 185 GeV. Similar results are obtained by the GFITTER collaboration, which quotes [5]:

$$m_h = 120.6_{-5.2[-6.2]}^{+17.0[+34.3]} \text{ GeV}, \quad (4)$$

based on all direct and indirect data, where both 1σ and 2σ error bars are given (the latter in the square brackets). The minimum χ^2 associated with the GFITTER fit is $\chi^2_{\min} = 17.82$ for 14 degrees of freedom.

3.3. Can a light Higgs boson be avoided?

If new physics beyond the Standard Model (SM) exists, then one expects shifts in the W and Z masses due to new contributions to the one-loop corrections. In many cases, these effects can be parameterized in terms of two quantities, S and T introduced by Peskin and Takeuchi [23]:

$$\bar{\alpha} T \equiv \frac{\Pi_{WW}^{\text{new}}(0)}{m_W^2} - \frac{\Pi_{ZZ}^{\text{new}}(0)}{m_Z^2}, \quad (5)$$

$$\frac{\bar{\alpha}}{4\bar{s}_Z^2\bar{c}_Z^2} S \equiv \frac{\Pi_{ZZ}^{\text{new}}(m_Z^2) - \Pi_{ZZ}^{\text{new}}(0)}{m_Z^2} - \left(\frac{\bar{c}_Z^2 - \bar{s}_Z^2}{\bar{c}_Z\bar{s}_Z} \right) \frac{\Pi_{Z\gamma}^{\text{new}}(m_Z^2)}{m_Z^2} - \frac{\Pi_{\gamma\gamma}^{\text{new}}(m_Z^2)}{m_Z^2}, \quad (6)$$

where $s \equiv \sin \theta_W$, $c \equiv \cos \theta_W$, and barred quantities are defined in the $\overline{\text{MS}}$ scheme evaluated at m_Z . The $\Pi_{V_a V_b}^{\text{new}}(q^2)$ are the new physics contributions to the one-loop gauge boson vacuum polarization functions. The region in the S - T plane consistent with precision electroweak data is shown in Fig. 1(a).

In order to avoid the conclusion of a light Higgs boson, new physics beyond the SM must enter at an energy scale between 100 GeV and 1 TeV. This new physics can be detected at the LHC

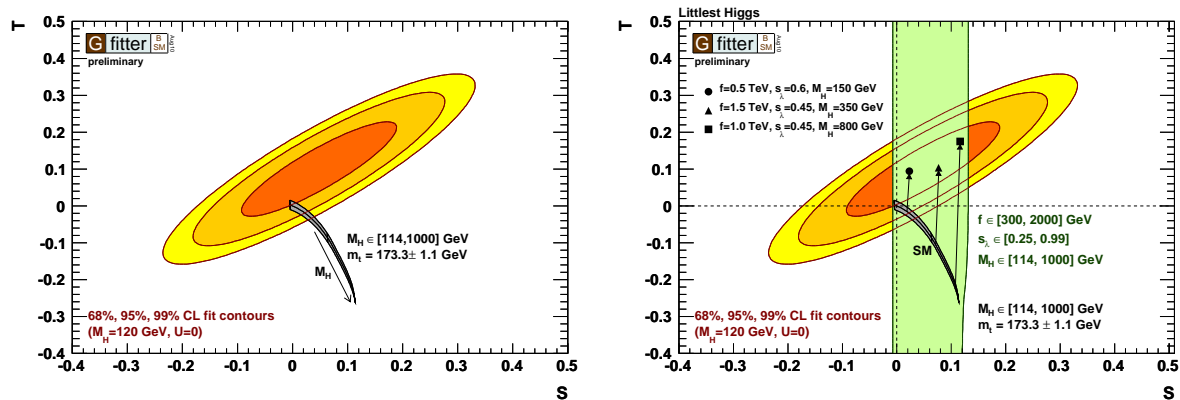


Figure 1. (a) In the left panel, the 68%, 95% and 99% CL contours in the S vs. T plane based on the GFITTER global Standard Model fit to electroweak precision data. The point $(S, T) = (0, 0)$ corresponds to $m_t = 173.1$ GeV and $m_h = 120$ GeV. (b) In the right panel, the GFITTER fit to electroweak precision data is exhibited for the littlest Higgs model of ref. [24] (with T -parity) for the parameters shown. Heavier Higgs masses are allowed, if the effects of the Higgs bosons to the gauge boson vacuum polarization functions are compensated by the effects due to new particles and interactions contained in the littlest Higgs model. Taken from ref. [5].

either through direct observation of new physics beyond the SM or by improved precision measurements at future colliders that can detect small deviations from SM predictions. Although the precision electroweak data is suggestive of a light Higgs boson, one cannot definitively rule out a significantly heavier Higgs boson if the new physics conspires to yield a total contribution to S and T that is consistent with the precision electroweak data [e.g., see Fig. 1(b)].

4. Prospects for Higgs discovery at the Tevatron

The Tevatron will continue to take data through the end of 2011. In addition to an increased integrated luminosity, there is still room for some improvements in the Higgs search analysis. The possibility of extending the Tevatron run by another three years is currently under discussion. To facilitate this discussion, a collaboration of Fermilab theorists and experimentalists produced a white paper making the case for an extended Run III of the Tevatron from the end of 2011 through 2014 [25]. The projected improvement of the Tevatron Higgs search is shown in Fig. 2.

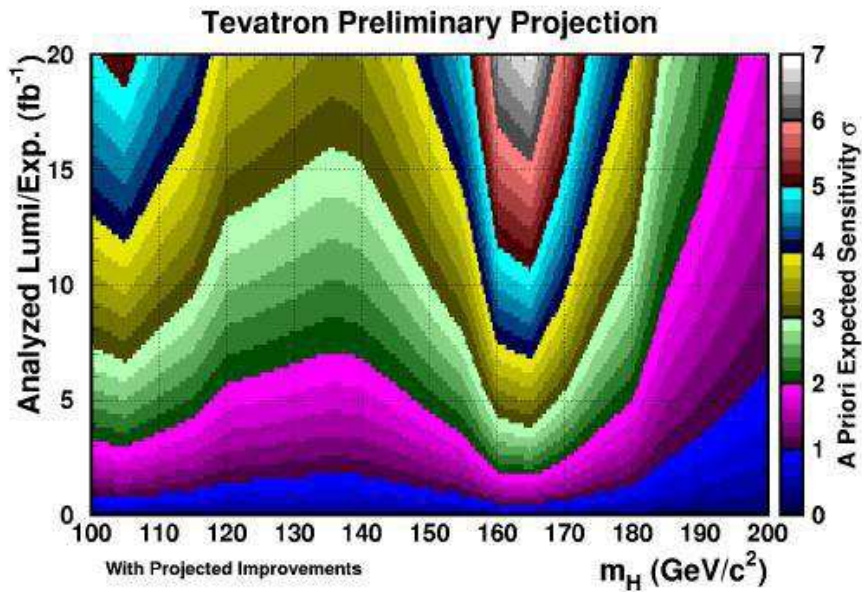


Figure 2. Higgs Boson sensitivity with projected improvements per experiment [25].

In Table 1, the expected sensitivity of the Tevatron Higgs search for Higgs masses of 115 GeV, 130 GeV and 145 GeV as a function of the analyzable luminosity per experiment is given.

Analyzable Lum/Exp	115 GeV	130 GeV	145 GeV
5 fb ⁻¹	2.2 σ	1.7 σ	1.9 σ
10 fb ⁻¹	3.1 σ	2.5 σ	2.7 σ
15 fb ⁻¹	3.8 σ	3.0 σ	3.2 σ
20 fb ⁻¹	4.4 σ	3.5 σ	3.7 σ

Table 1. Sensitivity to the Standard Model Higgs Boson combining all modes. The low mass ≤ 130 GeV mode is principally $q\bar{q} \rightarrow (W, Z) + (h \rightarrow b\bar{b})$; the higher mass ≥ 130 GeV mode is principally $gg \rightarrow h \rightarrow WW^*$. Taken from ref. [25].

5. Higgs phenomenology at the LHC

Although it is possible that evidence for the Higgs boson may emerge from future Tevatron running, the discovery of the Higgs boson and the identification of its properties are expected to take place at the LHC. Once the Higgs boson is discovered, a program of Higgs physics at the LHC must address the following important questions:

- How many Higgs states are there?
- Assuming one Higgs-like state is discovered,
 - is it a Higgs boson?
 - is it *the* SM Higgs boson?

The measurement of Higgs boson properties will be critical in order to answer the last two questions:

- mass, width, CP-quantum numbers (is the Higgs sector CP-violating?);
- branching ratios and Higgs couplings;
- reconstructing the Higgs potential (Higgs self-couplings).

5.1. Mechanisms for SM Higgs production at the LHC

At hadron colliders, the relevant Higgs production processes are shown in Fig. 3.

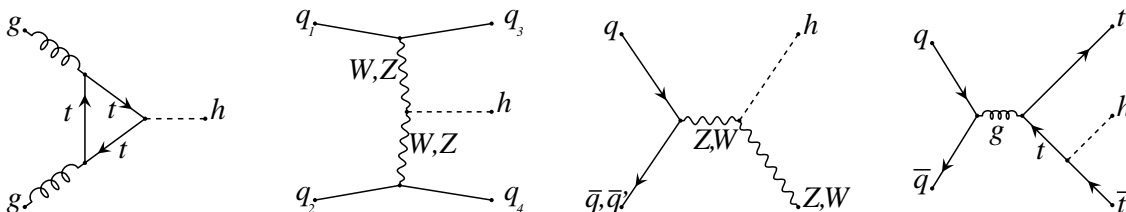


Figure 3. SM Higgs production mechanisms at hadron colliders

The Higgs boson is then detected via its decay products. The dominant channels for observing the Higgs boson at the LHC are:

$$\begin{aligned}
 gg &\rightarrow h^0, & h^0 &\rightarrow \gamma\gamma, VV^{(*)}, \\
 qq &\rightarrow qqV^{(*)}V^{(*)} \rightarrow qqh^0, & h^0 &\rightarrow \gamma\gamma, \tau^+\tau^-, VV^{(*)}, \\
 q\bar{q}^{(\prime)} &\rightarrow V^{(*)} \rightarrow Vh^0, & h^0 &\rightarrow b\bar{b}, WW^{(*)}, \\
 gg, q\bar{q} &\rightarrow t\bar{t}h^0, & h^0 &\rightarrow b\bar{b}, \gamma\gamma, WW^{(*)}.
 \end{aligned}$$

where $V = W$ or Z is a physical gauge boson and V^* is a virtual (off-mass-shell) gauge boson.

5.2. SM Higgs cross sections and branching ratios

The SM Higgs production cross-sections for $\sqrt{s} = 14$ TeV at the LHC are shown in Fig. 4. The discovery channels for Higgs production depend critically on the Higgs branching ratios. The branching ratios and total width of the SM Higgs boson are shown in Fig. 5.

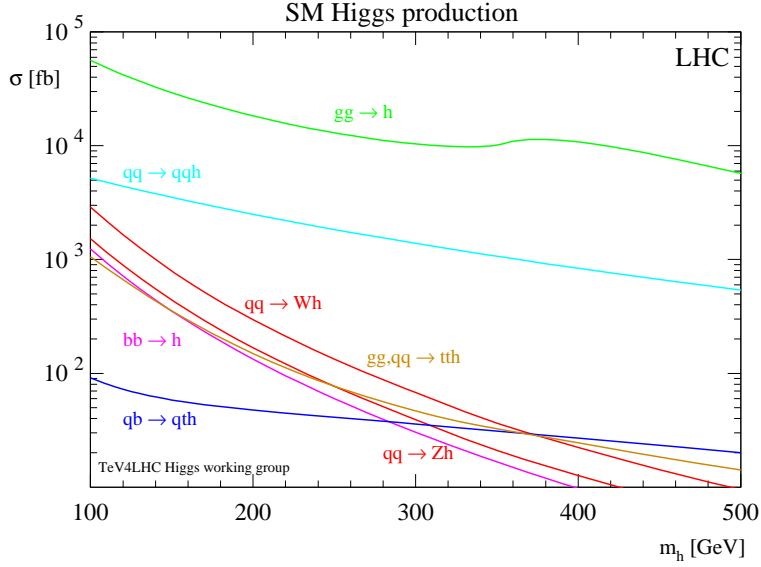


Figure 4. SM Higgs production cross-sections for $\sqrt{s} = 14$ TeV at the LHC (taken from ref. [26]).

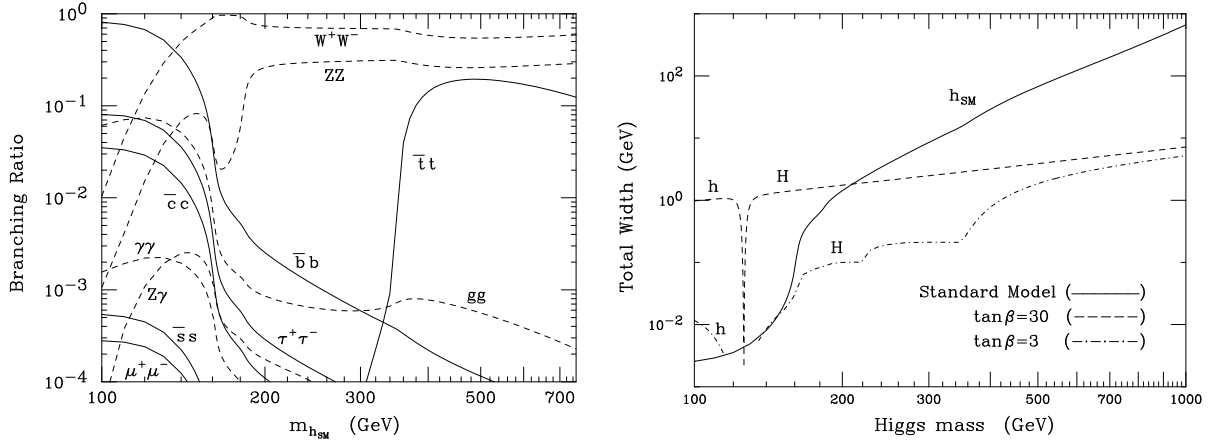


Figure 5. (a) In the left panel, the branching ratios of the SM Higgs boson are shown as a function of the Higgs mass. Two-boson [fermion-antifermion] final states are exhibited by solid [dashed] lines. (b) In the right panel, the total width of the Standard Model Higgs boson (denoted by h_{SM}) is shown as a function of its mass. For comparison, the widths of the two CP-even scalars, h^0 and H^0 of the MSSM are exhibited for two different choices of MSSM parameters ($\tan\beta = 3$ and 30 in the maximal mixing scenario; the onset of the $H^0 \rightarrow h^0 h^0$ and $H^0 \rightarrow t\bar{t}$ thresholds in the $\tan\beta = 3$ curve are clearly evident). Taken from ref. [10].

5.3. LHC prospects for SM Higgs discovery

An examination of Fig. 5 indicates that for $m_h < 135$ GeV, the decay $h \rightarrow b\bar{b}$ is dominant, whereas for $m_h > 135$ GeV, the decay $h \rightarrow WW^{(*)}$ is dominant (where one of the W bosons must be virtual if $m_h < 2m_W$). These two Higgs mass regimes require different search strategies. For the lower mass Higgs scenario, gluon-gluon fusion to the Higgs boson followed by $h \rightarrow b\bar{b}$ cannot be detected as this signal is overwhelmed by QCD two-jet backgrounds. Instead, the Tevatron

Higgs search employs associated production of the Higgs boson with a W or Z followed by $h \rightarrow b\bar{b}$. This process is more difficult at the LHC, where the signal-to-background discrimination is more severe. Instead, the LHC relies on the rare decay mode, $h \rightarrow \gamma\gamma$, which has a branching ratio of about 2×10^{-3} in the Higgs mass regime of interest. In the higher Higgs mass regime, both the Tevatron and the LHC rely primarily on $h \rightarrow WW^{(*)}$ for Higgs masses below 200 GeV. Should the Higgs mass be significantly larger than the current expectations based on precision electroweak data, then the LHC can discover the Higgs boson through the so-called golden channel, $h \rightarrow ZZ \rightarrow \ell^+\ell^-\ell^+\ell^-$.

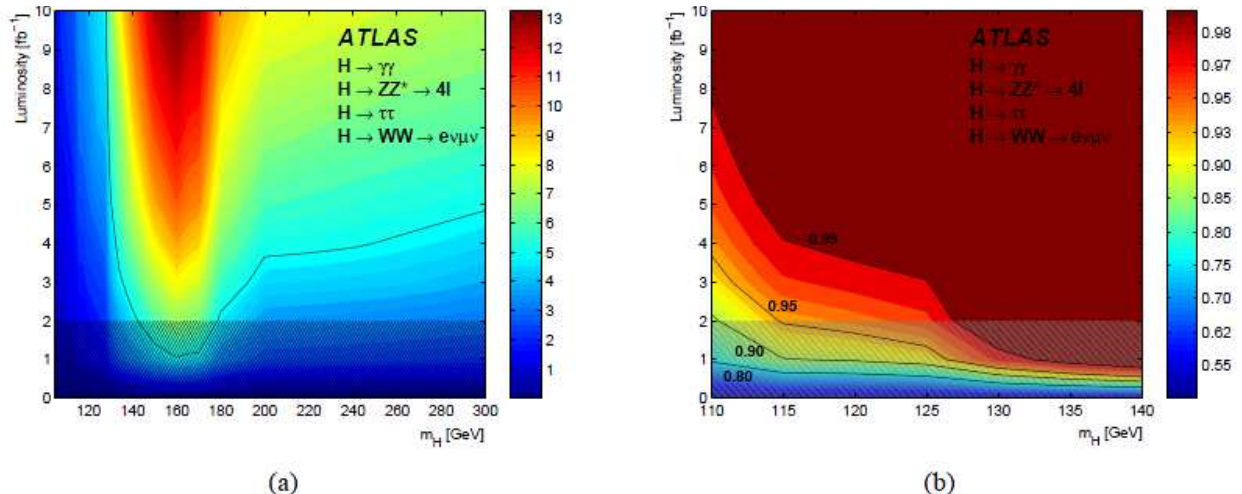


Figure 6. (a) The left panel depicts the significance contours for different SM Higgs masses and integrated luminosities. The thick curve represents the 5σ discovery contour. The median significance is shown with a color according to the legend. (b) The right panel depicts the expected luminosity required to exclude a Higgs boson with a mass m_H at a confidence level given by the corresponding color. In both panels, the hatched area below 2 fb^{-1} indicates the region where the approximations used in the combination are not accurate, although they are expected to be conservative. Taken from ref. [27].

The ATLAS projections [27] exhibited in Fig. 6 suggest that in the Higgs mass range of $114 \text{ GeV} \lesssim m_h \lesssim 130 \text{ GeV}$, the discovery of the Higgs (primarily through the rare $h \rightarrow \gamma\gamma$ decay mode) will require an integrated luminosity larger than 10 fb^{-1} at $\sqrt{s} = 14 \text{ TeV}$. The CMS projections [28] shown in Fig. 7 are slightly more optimistic in the low mass Higgs regime based on an “optimized” neural net analysis of the $h \rightarrow \gamma\gamma$ mode.

Currently, the LHC is running at half the design energy at significantly lower luminosities than those displayed in Figs. 6 and 7. Current projections suggest that at the end of 2011, the LHC running at $\sqrt{s} = 7 \text{ TeV}$ will accumulate a total integrated luminosity per experiment of about 1 fb^{-1} . Based on these projections, the ATLAS and CMS Higgs searches will yield a 5σ discovery in only a limited Higgs mass range, with a possible 95% exclusion over a somewhat larger Higgs mass range [29, 30]. As an example, Fig. 8 depicts the 95% Higgs mass exclusion region anticipated at the end of the 2011 run [29]. These results would likely match or even exceed the corresponding high mass ($m_h \geq 130 \text{ GeV}$) exclusion range expected from the Tevatron.

After the Higgs boson discovery, one must check that its properties are consistent with the theoretical expectations. Measurements of the spin, parity and couplings to gauge bosons and fermions typically need a large data sample (which requires tens to hundreds of fb^{-1}). However, in some special circumstances, one can discriminate between different hypotheses for spin and

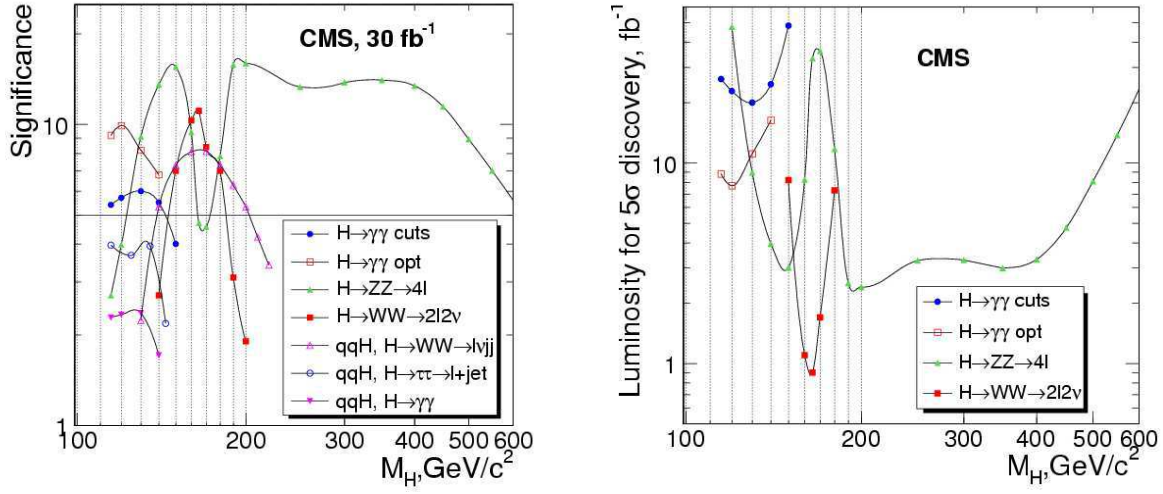


Figure 7. (a) The left panel depicts the signal significance as a function of the SM Higgs boson mass for 30 fb⁻¹ at $\sqrt{s} = 14$ TeV, for the different Higgs boson production and decay channels. (b) The right panel depicts the integrated luminosity required for a 5 σ discovery of the inclusive Higgs boson production, $pp \rightarrow h + X$, with the Higgs boson decay modes $h \rightarrow \gamma\gamma$, $h \rightarrow ZZ \rightarrow \ell^+\ell^-\ell^+\ell^-$ and $h \rightarrow W^+W^- \rightarrow \ell^+\nu_\ell \ell^-\bar{\nu}_\ell$. Taken from ref. [28].

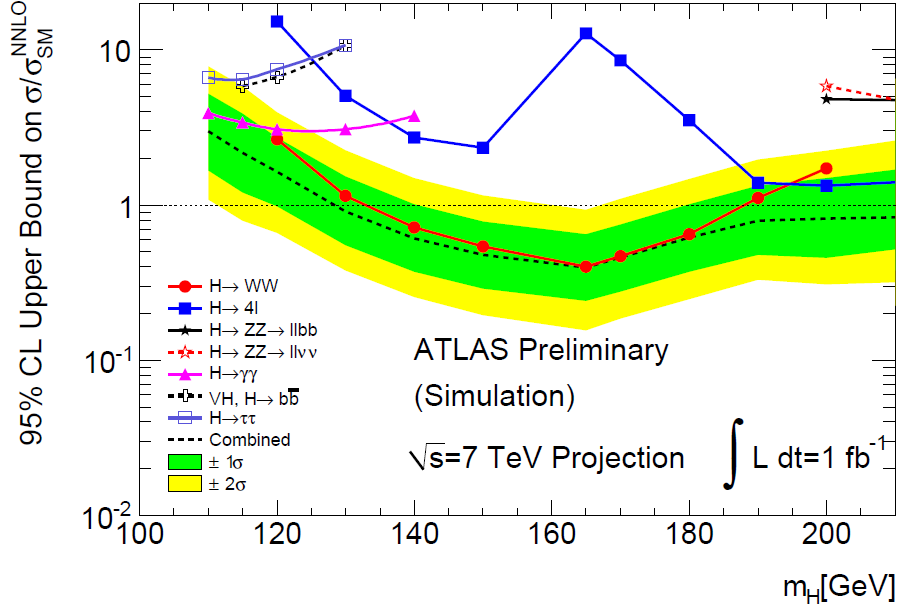


Figure 8. The multiple of the cross-section of a SM Higgs boson that can be excluded using 1 fb⁻¹ of data at $\sqrt{s} = 7$ TeV. At each mass, every channel giving reporting on it is used. The green and yellow bands indicate the range in which the limit is expected to lie, depending on the data. Taken from ref. [29]

$\mathbb{H}_0 \downarrow \mathbb{H}_1 \Rightarrow$	0^+	0^-	1^-	1^+
0^+	–	17	12	16
0^-	14	–	11	17
1^-	11	11	–	35
1^+	17	18	34	–

$\mathbb{H}_0 \downarrow \mathbb{H}_1 \Rightarrow$	0^+	0^-	1^-	1^+
0^+	–	52	37	50
0^-	44	–	34	54
1^-	33	32	–	112
1^+	54	55	109	–

Table 2. Minimum number of observed events such that the median significance for rejecting the null background-only hypothesis \mathbb{H}_0 in favor of the standard Higgs signal plus background hypothesis \mathbb{H}_1 (assuming \mathbb{H}_1 is right) exceeds 3σ and 5σ , respectively, with $m_H=145$ GeV. Based on an analysis of the $H \rightarrow ZZ^*$ decay mode. Taken from ref. [31].

parity with a small data sample. For example, for Higgs boson masses above about 130 GeV, it will be possible to isolate a data sample of $h \rightarrow ZZ^{(*)} \rightarrow \ell^+\ell^-\ell^+\ell^-$. By analyzing the distributions and correlations of the five relevant angular variables that describe the $\ell^+\ell^-\ell^+\ell^-$ events, one can achieve a median expected discrimination significance of 3σ with as few as 19 events for $m_h = 200$ GeV and even better discrimination for the off-shell decays of an $m_h = 145$ GeV Higgs boson [31], as shown in Table 2. Thus, if a Higgs boson is discovered at the LHC with 1 fb^{-1} , then it may already be possible to confirm a preference for the expected 0^+ spin-parity assignment with a small sample of Higgs events.

5.4. LHC prospects for MSSM Higgs discovery

In the decoupling limit, the properties of the lightest CP-even Higgs boson of the MSSM (denoted by h^0) are nearly identical to that of the SM Higgs boson. Thus, all the SM Higgs search techniques apply without modification in the MSSM. Moreover, the other MSSM Higgs bosons, H^\pm , H^0 and A^0 , which are significantly heavier than m_h (and m_Z), are roughly degenerate in mass (cf. Section 2.4). In the opposite limit (far from the decoupling limit), all physical MSSM Higgs bosons are typically below 200 GeV in mass and no single Higgs state possesses couplings that precisely match those of the SM Higgs boson [32].

Cross-sections and branching ratios for the MSSM Higgs boson (which depend on $\tan\beta$ as well as the corresponding Higgs mass) can be found in refs. [10, 14]. Here, we simply note that:

- gluon-gluon fusion can produce both neutral CP-even and CP-odd Higgs bosons.
- VV fusion ($V = W$ or Z) can produce only CP-even Higgs bosons (at tree-level). Moreover, in the decoupling limit, the heavy CP-even Higgs boson is nearly decoupled from the VV channel.
- Neutral Higgs bosons can be produced in association with $b\bar{b}$ and with $t\bar{t}$ in gluon-gluon scattering.
- Charged Higgs bosons can be produced in association with $t\bar{b}$ in gluon-gluon scattering.
- If $m_{H^\pm} < m_t - m_b$, then $t \rightarrow bH^-$ is an allowed decay, and the dominant H^\pm production mechanism is via $t\bar{t}$ production.
- Higgs bosons can be produced in pairs (e.g., H^+H^- , $H^\pm h^0$, $h^0 A^0$).
- Higgs bosons can be produced in cascade decays of SUSY particles.
- The total width of any one of the MSSM Higgs bosons is always $\lesssim 1\%$ of its mass [cf. Fig. 5(b)].
- Higgs search strategies depend on the location of the model in the m_A - $\tan\beta$ plane.

Simulations by the ATLAS and CMS collaborations shown in Fig. 9 exhibit which regions of the m_A - $\tan\beta$ plane are sensitive to the MSSM Higgs search. In particular, for large values

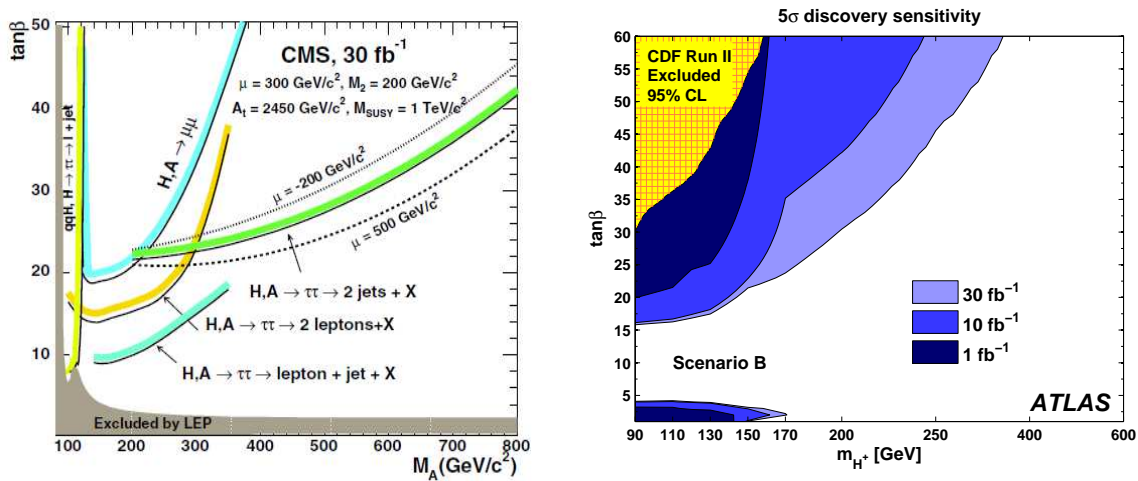


Figure 9. In the left panel, the 5σ discovery potential in the maximal mixing scenario for the heavy H^0 and A^0 scalars at CMS is shown for $\sqrt{s} = 14$ TeV and 30 fb^{-1} of data (taken from ref. [33]). In the right panel, the 5σ discovery sensitivity for the charged Higgs mass is shown as a function of m_{H^\pm} and $\tan\beta$ (taken from ref. [27]).

of $m_A \gtrsim 200$ GeV (corresponding to the decoupling limit), there is no sensitivity for the discovery of the heavy MSSM Higgs states, H^\pm , H^0 and A^0 , for moderate values of $\tan\beta$. This is the infamous “LHC wedge” region, in which the h^0 of the MSSM (whose properties are nearly indistinguishable from the SM Higgs boson) is the only MSSM Higgs boson that can be discovered at the LHC. Further details can be found in refs. [10, 14].

Acknowledgments

I would like to thank Jose Valle for providing me with the opportunity to visit Valencia and to speak at the PASCOS-2010 conference. I am especially grateful to Jose and his colleagues at the Universitat de València for their kind hospitality during my visit. I also appreciate a number of useful comments and suggestions from Sebastian Grab and Lorenzo Ubaldi, who read the draft version of this manuscript. This work is supported in part by the U.S. Department of Energy, under grant number DE-FG02-04ER41268.

References

- [1] P.W. Higgs, Phys. Rev. Lett. **12** (1964) 132; Phys. Rev. **145** (1966) 1156; F. Englert and R. Brout, Phys. Rev. Lett. **13** (1964) 321; G.S. Guralnik, C.R. Hagen, and T.W.B. Kibble, Phys. Rev. Lett. **13** (1964) 585.
- [2] S. Weinberg, Phys. Rev. D **13** (1976) 974; *ibid.* **19** (1979) 1277; L. Susskind, Phys. Rev. D **20** (1979) 2619.
- [3] J.F. Gunion, H.E. Haber, G.L. Kane and S. Dawson, *The Higgs Hunter’s Guide* (Westview Press, Boulder, CO, 2000).
- [4] The ALEPH, CDF, D0, DELPHI, L3, OPAL, SLD Collaborations, the LEP Electroweak Working Group, the Tevatron Electroweak Working Group, and the SLD Electroweak and Heavy Flavor groups, CERN-PH-EP/2009-023 (13 November, 2009); the most recent updated results can be found at <http://lepewwg.web.cern.ch/LEPEWWG/>.
- [5] H. Flacher, M. Goebel, J. Haller *et al.*, Eur. Phys. J. C **60** (2009) 543. [arXiv:0811.0009 [hep-ph]]; the most recent updated results can be found at <http://gfitter.desy.de/>.
- [6] H.P. Nilles, Phys. Rept. **110** (1984) 1; H.E. Haber and G.L. Kane, Phys. Rept. **117** (1985) 75; S.P. Martin, “A Supersymmetry Primer,” in *Perspectives on Supersymmetry II*, edited by G.L. Kane (World Scientific, Singapore, 2010) pp. 1–153 [arXiv:hep-ph/9709356v5].

- [7] E. Witten, Nucl. Phys. B **188** (1981) 513; L. Susskind, Phys. Rept. **104** (1984) 181.
- [8] For a recent review, see e.g., C.T. Hill, E. H. Simmons, Phys. Rept. **381** (2003) 235. [hep-ph/0203079].
- [9] B.A. Kniehl, Phys. Rept. **240** (1994) 211.
- [10] M. Carena and H.E. Haber, Prog. Part. Nucl. Phys. **50** (2003) 63 [arXiv:hep-ph/0208209].
- [11] A. Djouadi, Phys. Rept. **457** (2008) 1 [arXiv:hep-ph/0503172].
- [12] H.-S. Tsao, in *Proceedings of the 1980 Guangzhou Conference on Theoretical Particle Physics*, edited by H. Ning and T. Hung-yuan (Science Press, Beijing, 1980) p. 1240.
- [13] H.E. Haber and D. O’Neil, Phys. Rev. D **74** (2006) 015018 [arXiv:hep-ph/0602242]; Erratum–ibid. **74** (2006) 059905.
- [14] A. Djouadi, Phys. Rept. **459** (2008) 1 [arXiv:hep-ph/0503173].
- [15] H.E. Haber and R. Hempfling, Phys. Rev. Lett. **66** (1991) 1815; Y. Okada, M. Yamaguchi and T. Yanagida, Prog. Theor. Phys. **85** (1991) 1; J.R. Ellis, G. Ridolfi and F. Zwirner, Phys. Lett. B **257** (1991) 83.
- [16] See e.g., G. Degrossi, S. Heinemeyer, W. Hollik, P. Slavich and G. Weiglein, Eur. Phys. J. C **28** (2003) 133 [arXiv:hep-ph/0212020]; B.C. Allanach, A. Djouadi, J.L. Kneur, W. Porod and P. Slavich, JHEP **0409** (2004) 044 [arXiv:hep-ph/0406166]; S.P. Martin, Phys. Rev. D **75** (2007) 055005 [arXiv:hep-ph/0701051]; P. Kant, R.V. Harlander, L. Mihaila and M. Steinhauser, JHEP **1008** (2010) 104 [arXiv:1005.5709 [hep-ph]].
- [17] H.E. Haber and Y. Nir, Nucl. Phys. B **335** (1990) 363; J.F. Gunion and H.E. Haber, Phys. Rev. D **67** (2003) 075019 [arXiv:hep-ph/0207010].
- [18] R. Barate *et al.* [LEP Working Group for Higgs boson searches and ALEPH and DELPHI and L3 and OPAL Collaborations], Phys. Lett. B **565** (2003) 61. [hep-ex/0306033].
- [19] The TEVNPH Working Group for the CDF and D0 Collaborations, FERMILAB-CONF-10-257-E (July 28, 2010) [arXiv:1007.4587 [hep-ex]].
- [20] The ALEPH, DELPHI, L3 and OPAL Collaborations, and the LEP Higgs Working Group, LHWG Note 2001-04 (July 9, 2001); LHWG Note 2001-05 (July 4, 2001). Updates can be found at: <http://lep-higgs.web.cern.ch/LEPHIGGS/www/Welcome.html>.
- [21] D.A. Demir, Phys. Rev. D **60** (1999) 095007 [arXiv:hep-ph/9905571]; A. Pilaftsis and C.E.M. Wagner, Nucl. Phys. B **553** (1999) 3 [arXiv:hep-ph/9902371]; S.Y. Choi, M. Drees and J.S. Lee, Phys. Lett. B **481** (2000) 57 [arXiv:hep-ph/0002287]; M. Carena, J.R. Ellis, A. Pilaftsis and C.E.M. Wagner, Nucl. Phys. B **586** (2000) 92 [arXiv:hep-ph/0003180]; S. Heinemeyer, Eur. Phys. J. C **22** (2001) 521 [arXiv:hep-ph/0108059]; T. Ibrahim and P. Nath, Phys. Rev. D **63** (2001) 035009 [arXiv:hep-ph/0008237]; *ibid.* **66** (2002) 015005 [arXiv:hep-ph/0204092].
- [22] S. Schael *et al.* [The ALEPH, DELPHI, L3 and OPAL Collaborations, and the LEP Higgs Working Group], Eur. Phys. J. C **47** (2006) 547 [arXiv:hep-ex/0602042].
- [23] M.E. Peskin and T. Takeuchi, Phys. Rev. Lett. **65** (1990) 964; Phys. Rev. D **46** (1992) 381.
- [24] N. Arkani-Hamed, A.G. Cohen, E. Katz and A.E. Nelson, JHEP **0207** (2002) 034 [arXiv:hep-ph/0206021]; H.C. Cheng and I. Low, JHEP **0408** (2004) 061 [arXiv:hep-ph/0405243]; J. Hubisz, P. Meade, A. Noble and M. Perelstein, JHEP **0601** (2006) 135 [arXiv:hep-ph/0506042].
- [25] M. Carena *et al.*, “Run III: Continued Running of the Tevatron Collider Beyond 2011” (May 26, 2010), available from <http://beamdocs.fnal.gov/AD-public/DocDB/ShowDocument?docid=3617>.
- [26] U. Aglietti *et al.* [TeV4LHC Higgs Working Group], “Tevatron-for-LHC Report: Higgs,” FERMILAB-CONF-06-467-E-T [arXiv:hep-ph/0612172].
- [27] G. Aad *et al.* [The ATLAS Collaboration], *Expected Performance of the ATLAS Experiment: Detector, Trigger and Physics*, CERN-OPEN-2008-020 (December, 2008) [arXiv:0901.0512 [hep-ex]].
- [28] *CMS Physics Technical Design Report*, Volume II: Physics Performance, edited by A. De Roeck, M. Grünwald, J. Mnich, L. Pape and M. Spiropulu, CERN/LHCC 2006-021, CMS TDR 8.2 (26 June 2006).
- [29] The ATLAS Collaboration, *ATLAS Sensitivity Prospects for the Higgs Boson Production at the LHC Running at 7, 8 or 9 TeV*, ATLAS NOTE ATL-PHYS-PUB-2010-015 (October 27, 2010).
- [30] The CMS Collaboration, *The CMS physics reach for searches at 7 TeV*, CMS NOTE-2010/008 (July 20, 2010).
- [31] A. De Rujula, J. Lykken, M. Pierini, C. Rogan and M. Spiropulu, Phys. Rev. D **82** (2010) 013003 [arXiv:1001.5300 [hep-ph]].
- [32] E. Boos, A. Djouadi, M. Muhlleitner and A. Vologdin, Phys. Rev. D **66** (2002) 055004 [arXiv:hep-ph/0205160]; E. Boos, A. Djouadi and A. Nikitenko, Phys. Lett. B **578** (2004) 384 [arXiv:hep-ph/0307079].
- [33] S. Abdullin *et al.*, Eur. Phys. J. C **39**, s2 (2005) s41-s61.